All-Dielectric Self-Cloaked Structures

Z. Hayran* and H. Kurt

Nanophotonics Research Laboratory, TOBB University of Economics and Technology, Department of Electrical and Electronics
Engineering, Ankara, Turkey

R. Herrero, M. Botey, and K. Staliunas

Departament de Física, Universitat Politecnica de Catalunya (UPC), Barcelona, Spaiǹ

K. Staliunas

Institució Catalana de Recercai Estudis Avancats (ICREA), Barcelona, Spaiǹ

ABSTRACT: A general procedure to design objects that are intrinsically invisible (without the necessity of an external cloak) has not been demonstrated so far. Here we propose a flexible method to design such self-cloaked objects by uncoupling the scattered waves from the incident radiation via judiciously manipulating the scattering potential of the object. We show that such a procedure is able to yield optical invisibility for any arbitrarily shaped object within any specified frequency bandwidth by simply employing isotropic nonmagnetic dielectric materials, without the usage of loss or gain material. The validity of the design principle has been verified by direct experimental observations of the spatial electric field profiles and scattering patterns at the microwave regime. Our self-cloaking strategy may have profound implications especially in noninvasive probing, cloaked sensor applications, and scattering-free non-Hermitian optics based systems.

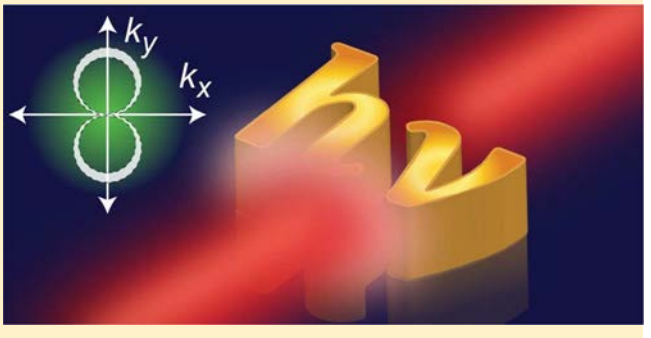

KEYWORDS: cloaking, scattering-cancellation, all-dielectric metamaterials

The deflection of a light ray from a straight path, known as light scattering, is one of the most common interactions between light and matter. As light impinges on an irregularity in space (e.g., object, particles, interface between two different media), it will experience partial reflection and transmission. While such phenomenon is responsible for creating marvelous light events in everyday life, such as the iridescent colors of butterfly wings, it may be desirable to cancel it for some applications. The so-called invisibility cloaking effect is a recent thought-provoking discovery, where the optical properties of the background and the object are tailored such that the light propagation mimics that of the free space, and thus, the object is effectively invisible to an external observer. A major breakthrough in 2006,[1,2] now known as transformation optics, has been achieved in this direction by deriving the spatial refractive index variation from the associated coordinate transformations required for a specific wave operation. Typically, to enable a cloaking effect with such a procedure, the physical space has to be distorted so that the incoming wave is rerouted around the object that is to be cloaked.[3−5] In effect, the distortion of the isotropic space results in an anisotropic and inhomogeneous index profile. Hence, due to the experimental burden of such a profile, various simplification attempts have been made to mitigate the fabrication requirements,[6−9] which, however, inevitably result in scarifying of the ideal cloaking performance.

Apart from transformation optics based cloaking design procedures, a technique called scattering cancellation may also be employed to render a particular object invisible. In this technique, a properly designed cover layer results in wave scattering that effectively cancels the scattering of the object.[10] In this regard, for instance, plasmonic covers,[11] multilayered dielectric coatings,[12] and acoustic surface impedances[13] have been shown to significantly reduce the scattering effect of an object.

Another completely different method to suppress the backscattered waves[14] and provide invisibility[15] has been recently proposed by employing the well-known Kramers−Kronig relations to relate the real and imaginary parts of a complex dielectric susceptibility profile. As such structures are already invisible per se, they do not require any external cloak

and are a promising tool especially for cloaked sensor applications.[16] However, these methods suffer from various drawbacks. First, as the susceptibility profile needs to be necessarily complex such that loss[14] or even gain[15] materials are required for a practical realization, which are often not easy to tailor in a bulk material. Second, the resultant susceptibility profile that is rendered invisible consists of an interface with infinitely extended tails rather than a specific object with a given shape and size. To form arbitrarily shaped self-cloaked objects, another study[17] suggested the usage of corrugated metallic wires. However, since the reported method relies on the resonant nature of the metallic wires, the self-cloaking effect has been demonstrated only for a narrow frequency bandwidth. Hence, broadband self-cloaked structures are yet to be elucidated and practically realized.

In this manuscript, we present a unique approach to achieve a self-cloaking effect (thus, not requiring any external cloak) for an arbitrary object within a specified frequency bandwidth and, in particular, propagation directions. We show how to obtain the required spatial index profile, which consists only of isotropic dielectric materials, that yields a scattering cancellation effect such that the object becomes cloaked, creating the illusion of restoring the original wavefront after leaving the object. We demonstrate this effect experimentally at the microwave regime by observing the spatial field profiles and by further investigating the frequency resolved scattering patterns.

DESIGN PRINCIPLE

The main idea of our proposal is based on the fact that the scattering behavior of a given object or, more generally, a spatial dielectric susceptibility distribution is associated with its spatial Fourier spectrum. We recently demonstrated and provided a generalized Hilbert transform on how this property can be exploited to tailor the scattering response of a given arbitrary object on a specific demand.[18] Here, to generate a cloaking effect and render a given object cloaked to the impinging electromagnetic radiation, all scatterings except in the incident direction should be canceled. Such a Fourier interpretation is briefly illustrated in Figure 1. Figure 1a depicts the spatial refractive index distribution n(x,y) of a given arbitrary object, whereas Figure 1b representatively shows the associated scattering potential $\tilde{\chi}(k_x, k_y)$, where k_x and k_y are the wavevectors along the x- and y-directions, respectively.

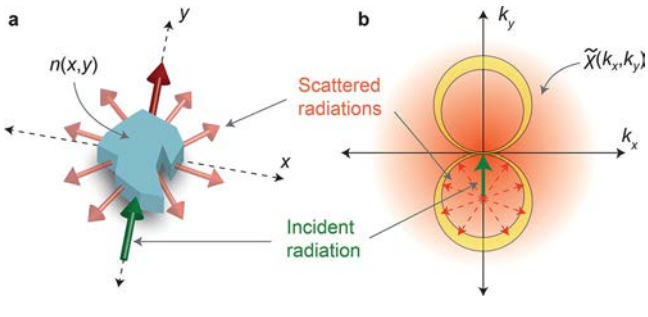

Figure 1. Scattering behavior of (a) a given object is determined by (b) its scattering potential and, thus, by a judicious inverse-design of the scattering potential one can eliminate undesired scattering directions (indicated by red dashed lines). For the cloaking effect all scattering directions except the incident direction are eliminated.

The scattering potential $\tilde{\chi}(k_x, k_y)$ can be defined as the twodimensional spatial Fourier transform of the dielectric susceptibility $\chi(x,y) = n^2(x,y) - 1$. As mentioned above, to eliminate all backward and forward scattered waves at a specific frequency, the Fourier components along a constant wavevector circle centered at the corresponding operational wavevector should be eliminated. On the other hand, to cancel the scattered waves for a specific frequency interval, the wavevector area (yellow colored areas in Figure 1b) between the corresponding two constant wavevector circles should be removed, as shown in Figure 1b. The removal of the particular regions in the scattering potential $\tilde{\chi}(k_x, k_y)$, in wavevector domain, uncouples the incident wavevector from given scattering directions. This is performed by using the invisibility wavevector region as a reciprocal band stop filter to the scattering potential. Optionally, after zeroing the wavevector regions, it is also possible to incorporate additional constraints in order to avoid extreme material parameters (e.g., index below one, as in Supporting Information, Supplementary Note 9). This is done by setting all such extreme material parameters to the specified limit value, and repeating the reciprocal filtering and constraint incorporation procedures until the resulting scattering potential involves the designated filtered wavevector regions. Finally, by taking the inverse Fourier transform of the resulting scattering potential, one would obtain the desired selfcloaked susceptibility profile.

Interesting to point out is that for a bidirectional cloaking effect, two symmetrically placed areas between constant wavevector circles should be removed. Since such a symmetry condition implies a purely real susceptibility when inverse Fourier transforming the scattering potential, the cloaked object would consist only of real refractive indices. In other words, no gain or loss materials would be required. Here, also important to note is that even though the presented method in Figure 1 relies on the Born approximation[14] (which requires very weak scattering and, hence, a low index contrast), we expect the operational principle to work also under large index differences. This is, in particular, due to fact that the spatial wavevector would not undergo a significant change when interacting with a scatterer that is designed to be cloaked (as the wave would propagate as in free space without any change in its spatial wavelength). Hence, the locations of the operational constant wavevector circles at the wavevector domain would remain almost constant and, in result, the Born approximation would be a good assumption even for scatterers with moderately large index contrasts, as will be demonstrated below.

EXPERIMENTAL ANALYSIS

To exemplify the proposed principle, we start with an object shaped in the letters "hv" whose refractive index profile n(x,y) and spatial dimensions are shown in Figure 2a. The scattering potential $\tilde{\chi}(k_x, k_y)$ of such an object is given in Figure 2b, which has been calculated as the Fourier transform of its dielectric susceptibility. Here, for demonstration purposes, we specify the positions of the inner and outer constant wavevector circles as $(k_x, k_y) = (0, \pm 2.60)$ cm^{-1} and $(0, \pm 3.10)$ cm^{-1}, respectively, whereas their radii are equal to 2.50 and 3.20 cm^{-1}, respectively, which result in a bidirectional cloaking effect in both the +y and the −y directions within the frequency interval of 10.5 and 12.9 GHz. The position and the wavevector circles have been determined so that the cloaking frequency interval and the material index range are within the ranges of our experimental equipment. Moreover, as opposed to Figure 1b, the wavevector region has a nonzero thickness at the center to efficiently eliminate the forward scattered waves. The field profile of the object has been numerically calculated via the finite-difference time-domain (FDTD) method[19] and given in Figure 2c, where the wavefront deformation can be clearly observed. By applying the above-mentioned procedure, the spatial index distribution, the scattering potential and the field profile would be obtained as in Figure 2d, e, and f, respectively. The field profile reveals the remarkable suppression of the scatterings and the nearperfect wavefront reconstruction. Important to note is that the index variation (and, hence, the index of the background) depends on the material to be used, similarly as in transformation optics based cloaking devices.[20] In the rest of this study, we have employed clear cast acrylic sheets to realize the original and cloaked objects to operate at the microwave regime. In this regard, the index variation presented in Figure 2 has been adjusted (by adding a constant index throughout the medium) to fit inside the index range realizable by perforated acrylic. Using such a material we have fabricated three structures: a reference structure consisting only of a background index (1.23), a structure with the original object (as in Figure 2a) and a structure with the cloaked object (as in Figure 2d). For a detailed description of the effective index calculation and the fabrication procedure see Supporting Information, Supplementary Note 1.

The experimental setup and the fabricated structures used to characterize the cloaking performance are shown in Figure 3a and b, respectively. As can be seen from Figure 3a, the experimental setup consists of a vector network analyzer (Agilent E5071C ENA), a motorized linear stage, a transmitter standard gain horn antenna, and a coaxial monopole antenna (for details of the measurement technique, please refer to the Supporting Information, Supplementary Note 2). The obtained spatial field distributions at the operational frequency 12.0 GHz are collectively given in Figure 4 for the +y and the −y directions, along with the corresponding numerical simulations.

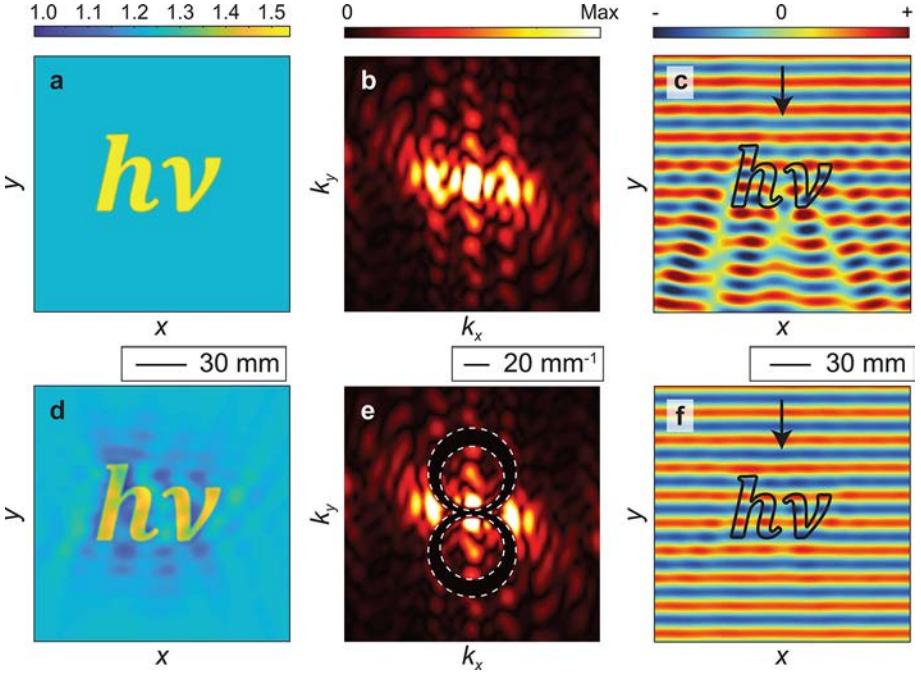

Figure 2. Refractive index distribution of (a) the initial object (exhibiting no cloaking effect) and (b) its associated scattering potential are given. The spatial electric field distribution of the initial object excited by a plane wave at 12.0 GHz is given in (c). After applying the cloaking procedure, the resultant cloaked refractive index profile and its scattering potential and field profile are depicted in (d), (e), and (f), respectively. The white dashed lines in (d) outline the filtered region in wavevector space. The background index is equal to 1.23. The black arrows indicate the direction of wave propagation and the black solid lines outline the object.

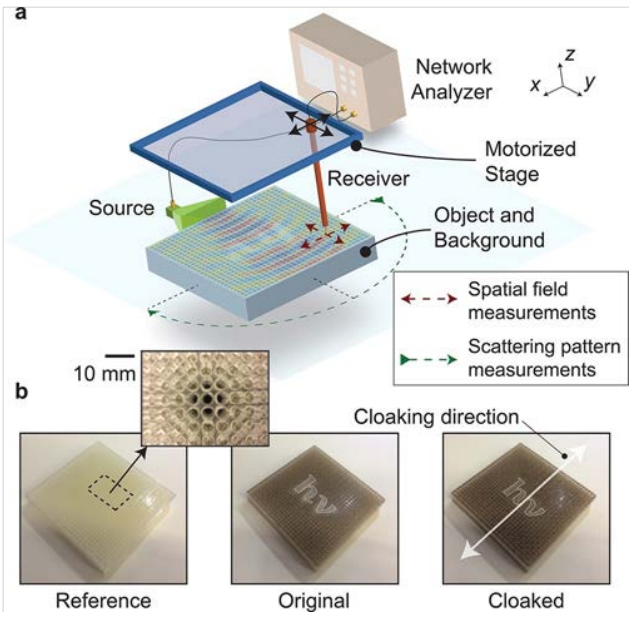

Figure 3. (a) Schematic illustration of the experimental setup. (b) Photographic view of the objects and the background that are engraved into clear cast acrylic (Plexiglas) sheets. From left to right: reference background structure without the object, original object and the resultant cloaked object. The white lines outline the object and the inset shows a zoomed portion of the perforated Plexiglas.

It follows from these figures that the original object (Figure 4b,e,h,k) causes light scattering and wave deformation, whereas the field propagation along the designed cloaked object (Figure 4c,f,i,l) mimics well that of the reference structures (Figure 4a,d,g,j). We should note that the cloaking performance is not perfect, which we mainly attribute to the discretization of the continuous index distribution. Moreover, another point worth mentioning is that the presented design principle assumes an incident wavevector in the +y or the −y direction, while the transmitter horn antenna radiates electromagnetic waves with spherical wavefronts. This might seem incongruous at first, however one should notice that the extended area of the filtered wavevector region (see Figure 2d) may also enable invisibility for grazing incidence angles. The reason for this is that, in the case of positioning, the constant wavevector circle at the regarding operational frequency with a grazing angle offset, the constant wavevector circle would still overlap with the filtered wavevector region, and thus, the scattered waves would be eliminated. We may attribute the slight discrepancy between numerical and experimental results in Figure 4 to the coupling effect of the receiver antenna′s metallic tip with the electromagnetic field along the structure. Such a coupling effect potentially distorts the field measurement especially when the detector is close to the structure. Besides, the evanescent tails of the propagating mode inside the structure decrease for a higher refractive index. Hence, in comparably higher refractive index regions the experimentally detected field amplitude is lower. This is especially noticeable around the center region (where the object is placed), see Figure 4, where the detected field amplitude is comparably lower precisely due to the high refractive index of the object. Furthermore, the field distributions for the +x and −x directions, for which the object does not exhibit invisibility, have also been measured and provided in Figure S2 (Supplementary Note 3). In addition, measured field distributions at the operational

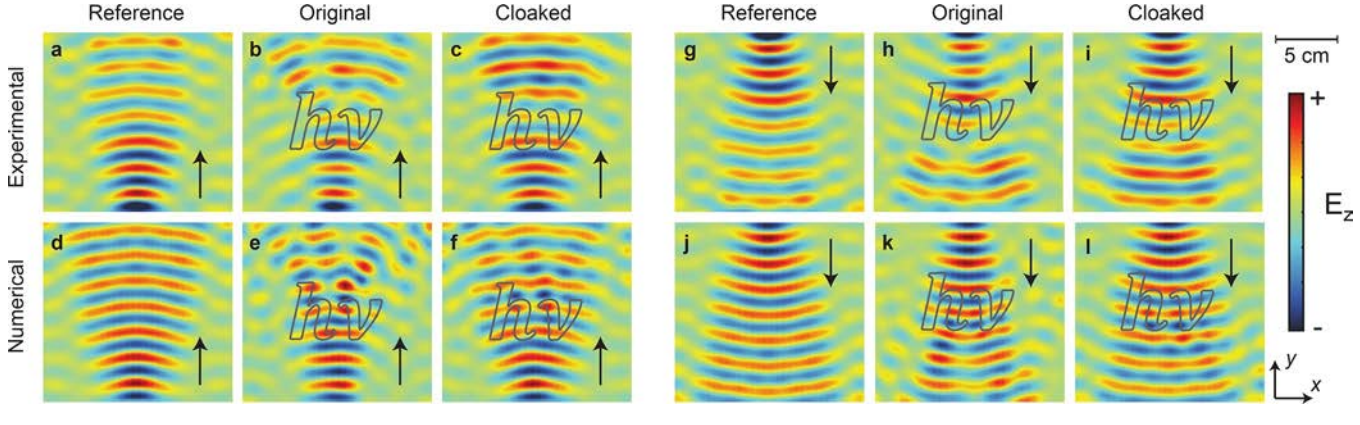

Figure 4. Measured and calculated field distributions for wave propagation in the +y (left) and −y (right) directions at the operational frequency 12.0 GHz. The first row shows the experimental results for the reference background (a, g), original object (b, h), and modified cloaked object (c, i), while the corresponding numerical simulations are depicted in the second row. Similar field measurements for the +x and −x directions, for which the modified object does not exhibit invisibility, and at the operational frequencies 10.5 and 12.9 GHz are provided in Figures S3, S4, and S5, respectively (see Supplementary Note 3). The black arrows reveal the direction of wave propagation, while the gray lines outline the boundaries of the "hν" shaped object. Moreover, the time evolutions of the measured field profiles are provided in Supplementary Video (SI). All figures share the same 5 cm scale bar.

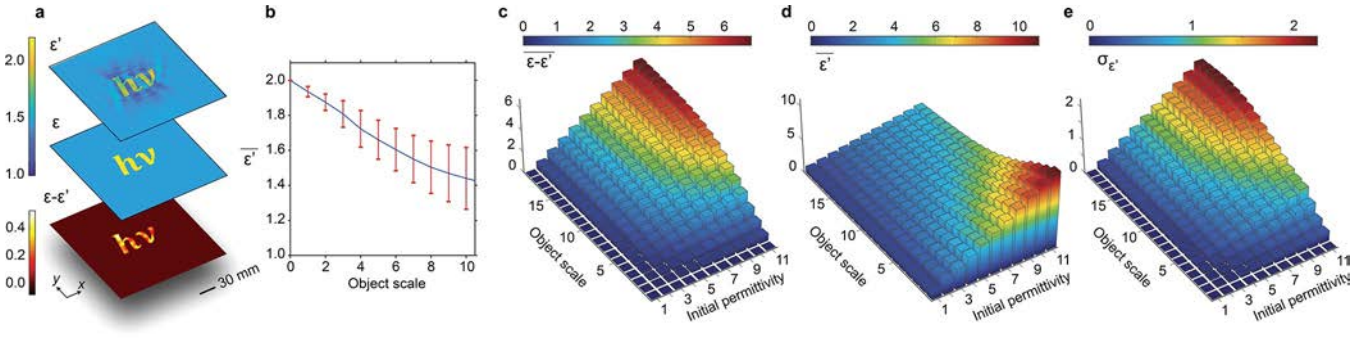

Figure 6. (a) From top to down: spatial permittivity profile of the cloaked object; spatial permittivity profile of the original object; the difference of the spatial permittivity profiles inside the object region of the cloaked (ε′) and original (ε) structure. (b) The mean value of the permittivity profile inside the object region of the cloaked structure (ε′) is shown. The initial permittivity of the object equals to 2. The object scale parameter has been defined with respect to the original size presented in (a). The "error" bars represent the standard deviation from the mean permittivity values. (c) The mean value of the permittivity perturbation ε−ε′, (d) the mean value of ε′, and (e) the standard deviation of ε′ is given with respect to the initial permittivity and object size. The mean values and standard deviations have been calculated spatially along the permittivity profiles inside the object region. In all cases, the procedure is applied to induce a self-cloaking effect in the operational bandwidth of 10.5−12.9 GHz.

frequencies 10.5 and 12.9 GHz have been provided in Figures S3 and S4, respectively (Supplementary Note 3).

To quantitatively compare the spectrally resolved scattering pattern of the original and the cloaked object, the electric field has been measured rotationally around all three structures with a distance of 135.0 mm with respect to the center of the structures (as indicated by green dashed lines in Figure 3a). To account only for the scattered waves induced by the object, the scattering caused by the diffraction effect of the finite slab structure should be excluded. For this, the scattered electric field values of the reference structure has been subtracted from that of the cloaked and original structures and the absolute values of the differences were taken. Furthermore, the results were normalized by the field spectra obtained without the structures.

Figure 5a and b show the obtained scattering plots for the original and the cloaked objects, respectively; for wave propagation in the +y direction. It can be inferred from these figures that the scattered amplitude decreases substantially in the designed cloaking frequency interval (indicated by black dashed lines) for the cloaked object, as expected. It further follows from these figures that the scattering is not perfectly diminished, which we attribute to the fabrication disorders and to the coupling effect of the receiver antenna with the scattered field. One interesting fact to notice is that for frequencies lower than the designed cloaking frequency interval, the scattered amplitude remains also near zero. We attribute this observation to the fact that the forward-scattering Fourier components along constant wavevector circles, corresponding to lower frequencies, are already included in the filtered wavevector region. In other words, as these constant wavevector circles have a smaller radii, the tangential overlap at the forwardscattering Fourier region between them and the filtered region becomes larger, as compared to high-frequency constant wavevector circles. In particular, this makes our proposed method distinct from previously demonstrated cloaking procedures, where the cloaking performance is rapidly degraded away from the central frequency or even drastically enhanced scatterings are observed in nearby regions of the operational bandwidth.[21] Similar scattering plots for other propagation directions have been prepared in Figure S5 (Supplementary Note 4), where an analogous scattering suppression can be observed for wave propagation in the opposite (−y) direction. Furthermore, to allow also for an experimental observation of the phase-front response, a broadband scanning of the electric field was performed at the back face of the structures. The experimental setup and the results of these measurements are provided in Figures S6 and S7, respectively (Supplementary Note 5), where one can similarly observe the scattering suppressions and wavefront reconstructions in the designated frequency range.

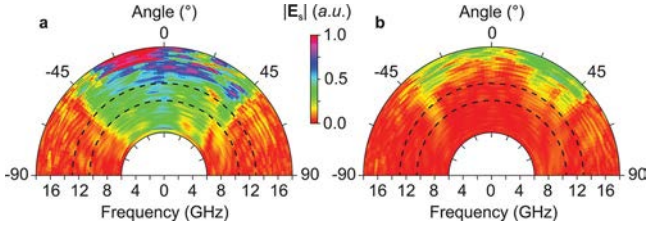

Figure 5. Measured angular scattered field (E_s) amplitude distributions for the (a) original object and (b) the modified cloaked object. Wave propagation is in the +y direction. The scattering angle is always in the same x−y plane and is defined with respect to the vertical y-axis in clockwise direction. The dashed black lines indicate the frequency range for which the object is designed to be cloaked. Similar scattering plots for other incidence directions are provided in Figure S5 (Supplementary Note 4).

REQUIRED INDEX PERTURBATION FOR SELF-CLOAKING

Finally, we would like to address the level of index perturbation in response to applying the proposed procedure. Although the proposal is ideally suited for designing self-cloaked objects, rather than designing a cloak to an existing object, it would be elucidative to analyze the amount of permittivity deviation along the object from the initial reference value. In this regard, Figure 6a shows the permittivity profiles of the cloaked and original structure, and the permittivity perturbation occurring along the object region. Figure 6b shows the spatial mean values of the permittivity inside the cloaked object region, where the initial permittivity of the cloaked object corresponds to 2. Furthermore, while Figure 6c presents the mean value of the permittivity distribution, Figure 6d and e show the mean values and the standard deviations of the permittivity along the cloaked object region, respectively. It follows from these figures that the permittivity perturbation along the object region increases with the initial permittivity and object size. Moreover, one can deduce that, with increasing object size and permittivity, the mean value of the permittivity along the object region deviates from the initial permittivity value, while the standard deviation from the mean value increases. Specifically, we see that, especially for large objects, the permittivity deviation from the initial value becomes significant.

However, we should note that for most photonic applications the size of the object is on the order of the operational wavelength. Since in such typical photonic structures the required index deviation from the initial value is not typically high, the resulting structure can be experimentally realized with a single material having varying local filling ratios (as shown in the previous section). Nevertheless, for larger objects the proposed concept can be implemented with a set of multiple materials. Moreover, we should note that although the resulting mean permittivity values are typically lower than the initial reference value, the resulting permittivity value can be scaled to around its initial reference value. Since, the reciprocal domain would not be distorted through multiplication or addition of a constant value, the scaled permittivity profiles would still be inherently cloaked.

CONCLUSIONS

In this manuscript, we have provided a general description on how to achieve a self-cloaking effect for a given object with arbitrary shape and dimensions by merely using isotropic dielectric materials. We demonstrated the feasibility of the proposed method by experimental analyses conducted at the microwave regime. Since the proposed method is independent from spatial dimensions, the same procedure can be applied to realize the proposed invisibility-based cloaking effect at the micro- or nanoscale (see Supplementary Note 6), as such fabrication methods are already matured owing to the extensive research effort in the field of transformation optics.[22,23] Moreover, in principle, the self-cloaking effect can be also extended to operate under broad-angle incidence (or even omnidirectionally, as shown in Supplementary Note 7), if the scattered waves are also eliminated for such a broad incidence angle range. We note that the design principle is still valid in the presence of material absorption (see Supplementary Note 8) and for higher refractive index contrasts (see Supplementary Note 9). Finally, as demonstrated in Supplementary Note 10, we would like to highlight the fact that the proposed method can be also used to induce a unidirectional cloaking effect by straightforwardly extending the idea to complex non-Hermitian profiles.[24] The presented work provides a new perspective in the field of optical cloaking, and may be especially valuable for "sensor cloaking"[16] applications and non-Hermitian optics based systems.

ASSOCIATED CONTENT

* Supporting Information

The Supporting Information is available free of charge on the ACS Publications website at DOI: 10.1021/acsphotonics.7b01608.

Supplementary note: Information and discussion on the calculation of the effective index and the fabrication of the acrylic slabs, the experimental measurement technique, further measured spatial field distributions, the scattered intensity plots, the measurement of the electric field spectra, non-Hermitian unidirectional cloaking, possible experimental implementation at the visible regime, the extension to omnidirectional cloaking, self-cloaking in the presence of material absorption, and self-cloaking with high refractive index materials (PDF).

Supplementary video: Time evolutions of the measured spatial field profiles at 12.0 GHz (AVI).

AUTHOR INFORMATION

Corresponding Author

*E-mail: zekihayran@etu.edu.tr; zekihayran.etu@gmail.com. Phone: +(90) 312 292 45 87.

Notes

The authors declare no competing financial interest.

ACKNOWLEDGMENTS

Authors gratefully acknowledge financial support of NATO SPS Research Grant No. 985048; Spanish Ministerio de Ciencia e Innovacion and European Union FEDER Project FIS2015-65998-C2-1-P. H.K. also acknowledges partial support of the Turkish Academy of Science.

REFERENCES

(1) Leonhardt, U. Optical Conformal Mapping. Science 2006, 312 (5781), 1777−1780.

(2) Pendry, J. B.; Schurig, D.; Smith, D. R. Controlling Electromagnetic Fields. Science 2006, 312 (5781), 1780−1782.

(3) Chen, H.; Chan, C. T.; Sheng, P. Transformation Optics and Metamaterials. Nat. Mater. 2010, 9 (5), 387−396.

(4) Zhang, B. Electrodynamics of Transformation-Based Invisibility Cloaking. Light: Sci. Appl. 2012, 1, e32.

(5) Zheng, B.; Madni, H. A.; Hao, R.; Zhang, X.; Liu, X.; Li, E.; Chen, H. Concealing Arbitrary Objects Remotely with Multi-Folded Transformation Optics. Light: Sci. Appl. 2016, 5 (12), e16177.

(6) Schurig, D.; Mock, J. J.; Justice, B. J.; Cummer, S. A.; Pendry, J. B.; Starr, A. F.; Smith, D. R. Metamaterial Electromagnetic Cloak at Microwave Frequencies. Science 2006, 314 (5801), 977−980.

(7) Yan, M.; Ruan, Z.; Qiu, M. Cylindrical Invisibility Cloak with Simplified Material Parameters Is Inherently Visible. Phys. Rev. Lett. 2007, 99 (23), 113903.

(8) Chen, H.; Liang, Z.; Yao, P.; Jiang, X.; Ma, H.; Chan, C. T. Extending the Bandwidth of Electromagnetic Cloaks. Phys. Rev. B: Condens. Matter Mater. Phys. 2007, 76 (24), 241104.

(9) Ma, H. F.; Cui, T. J. Three-Dimensional Broadband GroundPlane Cloak Made of Metamaterials. Nat. Commun. 2010, 1, 1.

(10) Chen, P. Y.; Soric, J.; Alu, A. Invisibility and Cloaking Based on Scattering Cancellation. Adv. Mater. 2012, 24, OP281−OP304.

(11) Rainwater, D.; Kerkhoff, A.; Melin, K.; Soric, J. C.; Moreno, G.; Alu, A. Experimental Verification of Three-Dimensional Plasmonic Cloaking in Free-Space. New J. Phys. 2012, 14, 013054.

(12) Wang, X.; Semouchkina, E. A Route for Efficient NonResonance Cloaking by Using Multilayer Dielectric Coating. Appl. Phys. Lett. 2013, 102 (11), 113506.

(13) Chen, P. Y.; Farhat, M.; Guenneau, S.; Enoch, S.; Alu, A. Acoustic Scattering Cancellation via Ultrathin Pseudo-Surface. Appl. Phys. Lett. 2011, 99 (19), 191913.

(14) Horsley, S. A. R.; Artoni, M.; La Rocca, G. C. Spatial KramersKronig Relations and the Reflection of Waves. Nat. Photonics 2015, 9 (7), 436−439.

(15) Longhi, S. Bidirectional Invisibility in Kramers-Kronig Optical Media. Opt. Lett. 2016, 41 (16), 3727.

(16) Alu, A.; Engheta, N. Cloaking a Sensor. Phys. Rev. Lett. 2009, 102 (23), na.

(17) Ye, D.; Lu, L.; Joannopoulos, J. D.; Soljacič , M.; Ran, L. Invisiblé Metallic Mesh. Proc. Natl. Acad. Sci. U. S. A. 2016, 113 (10), 2568− 2572.

(18) Hayran, Z.; Herrero, R.; Botey, M.; Kurt, H.; Staliunas, K. Invisibility on demand based on a generalized Hilbert transform. arXiv:1703.09490 [physics.optics] arXiv preprint 2017, na.

(19) Lumerical Solutions, Inc. software. http://www.lumerical.com/tcad-products/fdtd/.

(20) Gharghi, M.; Gladden, C.; Zentgraf, T.; Liu, Y.; Yin, X.; Valentine, J.; Zhang, X. A Carpet Cloak for Visible Light. Nano Lett. 2011, 11 (7), 2825−2828.

(21) Monticone, F.; Alu, A. Invisibility Exposed: Physical Bounds on Passive Cloaking. Optica 2016, 3 (7), 718.

(22) Xu, X.; Feng, Y.; Hao, Y.; Zhao, J.; Jiang, T. Infrared Carpet Cloak Designed with Uniform Silicon Grating Structure. Appl. Phys. Lett. 2009, 95 (18), 184102.

(23) Gabrielli, L. H.; Cardenas, J.; Poitras, C. B.; Lipson, M. Silicon Nanostructure Cloak Operating at Optical Frequencies. Nat. Photonics 2009, 3 (8), 461−463.

(24) Guo, A.; Salamo, G. J.; Duchesne, D.; Morandotti, R.; VolatierRavat, M.; Aimez, V.; Siviloglou, G. A.; Christodoulides, D. N. Observation of PT-Symmetry Breaking in Complex Optical Potentials. Phys. Rev. Lett. 2009, 103 (9), 093902.